SOI: 1.1/TAS DOI: 10.15863/TAS
International Scientific Journal
Theoretical & Applied Science

p-ISSN: 2308-4944 (print) **e-ISSN:** 2409-0085 (online)

Year: 2025 **Issue:** 12 **Volume:** 152

Received: 27.12.2025
Accepted/Published: 30.12.2025
https://T-Science.org

Issue Article

Denis Chemezov
Vladimir Polytechnic College
MEng, Honorary Worker of the Education Field of the Russian Federation, Academician of International Academy of Theoretical and Applied Sciences, Lecturer, Russian Federation
https://orcid.org/0000-0002-2747-552X
vpk-science@yandex.ru

Aleksandr Burkov
Vladimir Polytechnic College
Student, Russian Federation

Ekaterina Suslova
Vladimir Polytechnic College
Student, Russian Federation

Yaroslav Baranov
Vladimir Polytechnic College
Student, Russian Federation

Valeriy Gogulin
Vladimir Polytechnic College
Student, Russian Federation

Ilyas Evstigneev
Vladimir Polytechnic College
Student, Russian Federation

Sergey Bezrukov
Vladimir Polytechnic College
Student, Russian Federation

Sergey Nizov
Vladimir Polytechnic College
Student, Russian Federation

APPLICATION OF THE FINITE ELEMENT METHOD FOR QUALITATIVE ASSESSMENT OF THE STRESS-STRAIN STATE OF A STEEL WORKPIECE DURING FLAT GRINDING

***Abstract**: This article presents the results of computer modeling of the flat grinding process of 1010 low-carbon steel, in order to assess the stress-strain state of the workpiece being processed. By applying the properties to the models of the workpiece and the grinding wheel, the calculated values of von Mises stress and material pressure were obtained, which can be taken into account in real production. The coefficient of volumetric strain determines the areas of tensile and compressive deformation of the material being ground, and how they affect the quality and accuracy of the processed surface.*

Key words: *grinding, grinding wheel, workpiece, stress-strain state, model.*

Language: *English*

Citation: Chemezov, D., et al. (2025). Application of the finite element method for qualitative assessment of the stress-strain state of a steel workpiece during flat grinding. *ISJ Theoretical & Applied Science, 12 (152)*, 75-80.

Soi: https://s-o-i.org/1.1/TAS-12-152-14 ***Doi***: https://dx.doi.org/10.15863/TAS.2025.12.152.14

Scopus ASCC: *2209.*

1. Introduction

Flat grinding is used for the final profiling of workpiece planes in order to achieve the required accuracy and quality of the surfaces [1-2].

During flat grinding of a metal workpiece with a grinding wheel, localized plastic deformation, residual stresses, and elastic deformations occur in the workpiece material [3-9]. As material is removed from the workpiece, tensile stresses are generated in front of the grinding zone, while compressive stresses are generated under the surface of the workpiece, affecting the structural integrity and surface quality of the finished product. The intensity of these stresses will depend on factors such as the grinding modes, the properties of the workpiece and the grinding wheel, and the temperature gradient distribution in the cutting zone, which ultimately affect the distribution of residual stresses, the microstructure, and the likelihood of surface or subsurface cracks.

The most effective method for quantifying the stress-strain state of the material of the workpiece being ground is finite element modeling of the process. Flat grinding simulation involves creating a detailed representation of the grinding process to optimize parameters such as the choice of abrasive wheel, feed rate, flow rate, and cooling type to achieve high-quality surface finish [10]. This typically involves modeling the contact between the grinding wheel and the workpiece, analyzing heat generation, material removal rates, and surface integrity. Using this method, the flat grinding process of structural steel was simulated in this study, and a qualitative assessment of stresses and deformations that occur in the material was performed to determine the accuracy of the processed surface of the workpiece.

2. Materials and methods

The Comsol Multiphysics 5.6 software product's multi-body dynamics module was used to simulate the flat grinding process of a steel workpiece. The calculation was performed in a two-dimensional setting with the specified boundary conditions of the experiment.

The workpiece model was a rectangle 3 m long and 1 m high. A 1-meter-radius grinding wheel model was built over the workpiece model. The periphery of the grinding wheel model was 0.1 mm lower than the workpiece model's surface, setting the grinding depth. The accuracy of the calculation results visualization was determined by dividing the models into 2708 finite elements with an average element quality of 0.9802. The orientation of the workpiece and grinding wheel models during flat grinding and the mesh on the models are shown in the Figure 1.

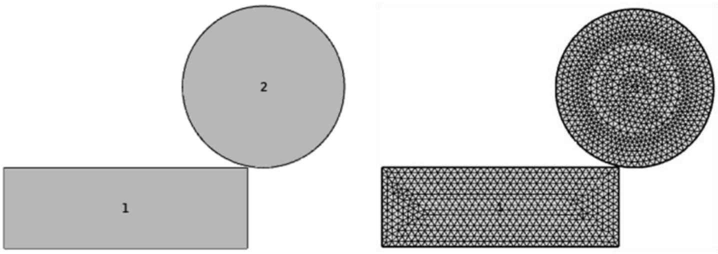

a *b*

Figure 1. Conditions for modeling the flat grinding process: *a* – models of workpiece *1* and grinding wheel *2*; *b* – mesh on the models.

The lower flat surface of the workpiece model was rigidly fixed. The grinding wheel model moved along the *X*-axis at a speed of 5 m/min and rotated around its axis at a speed of 1800 rpm. The contact between the grinding wheel model and the unfixed horizontal plane of the workpiece model was calculated using the penalty method for dynamic contact in numerical simulation.

The properties of 1010 steel and silicon carbide were assigned to the workpiece and grinding wheel models, respectively. 1010 low-carbon steel is a linearly elastic material, while silicon carbide has the properties of an anisotropic material. Since the temperature in the contact zone between the grinding wheel and the workpiece varies between 500 and 800°C, the change in material properties must be taken into account when the temperature load varies.

The properties of the workpiece material and the grinding wheel material, depending on the temperature, are presented in the Figures 2 and 3.

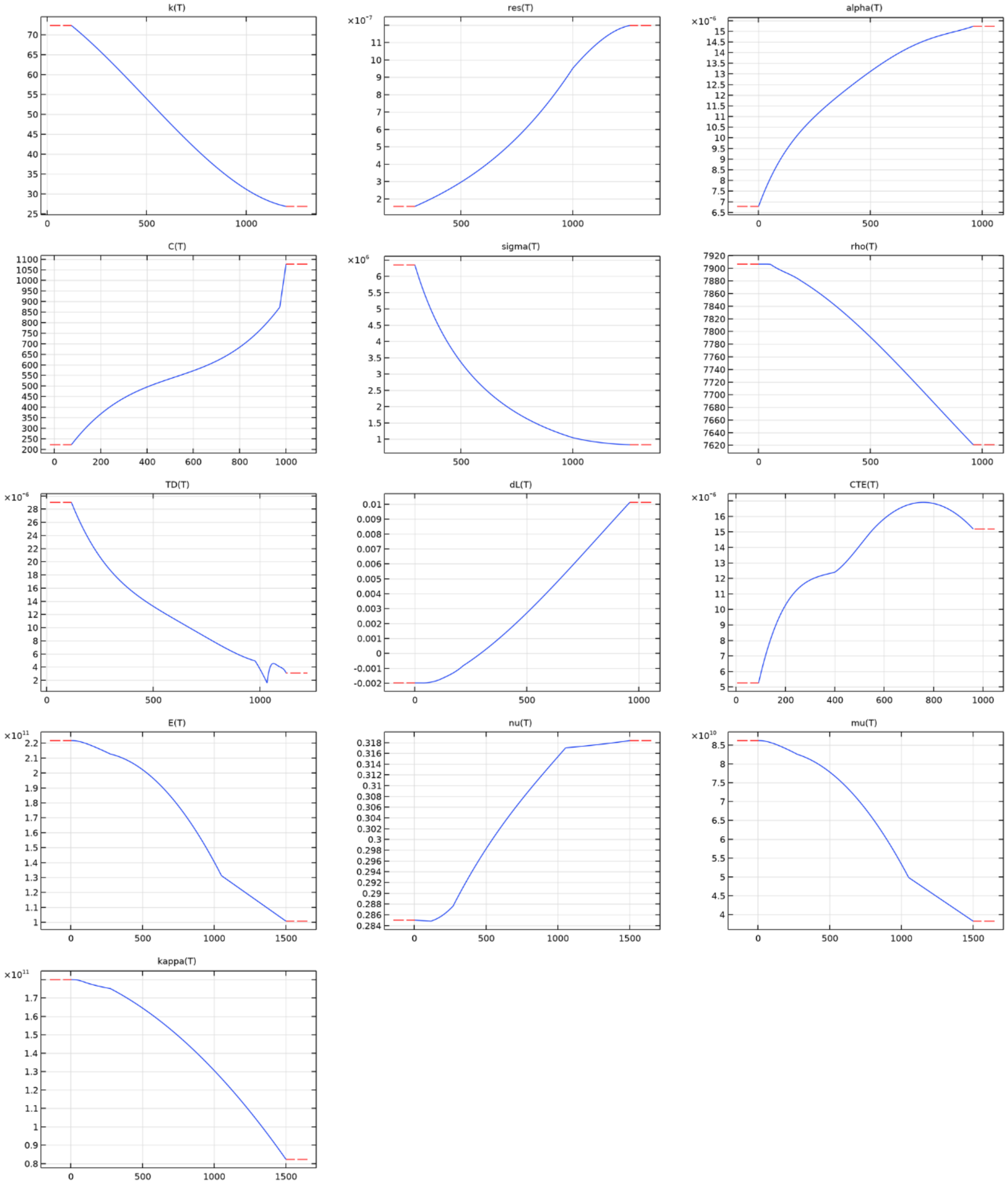

Figure 2. Properties of 1010 steel (workpiece) depending on temperature changes: *T* – temperature, *k* – thermal conductivity, *res* – resistivity, *alpha* – coefficient of thermal expansion, *C* – heat capacity at constant pressure, *sigma* – electrical conductivity, *rho* – density, *TD* – thermal diffusivity, *dL* – thermal strain, *CTE* – tangent coefficient of thermal expansion, *E* – Young's modulus, *nu* – Poisson's ratio, *mu* – shear modulus, *kappa* – bulk modulus.

Based on the analysis of the dependence graphs, the following conclusions were made:

1. For 1010 steel, it is characteristic to increase the value of resistivity, coefficient of thermal expansion, heat capacity at constant pressure, thermal strain, tangent coefficient of thermal expansion, and Poisson's ratio, and to decrease the value of thermal conductivity, electrical conductivity, density, thermal diffusivity, Young's modulus, shear modulus, and bulk modulus with an increase in the temperature in the grinding zone.

2. Silicon carbide is characterized by an increase in yield stress, coefficient of thermal expansion, heat capacity at constant pressure, electrical conductivity, molar heat capacity, normal total emissivity, and thermal strain, as well as a decrease in thermal conductivity, density, and thermal diffusivity, and a constant value of resistivity with an increase in temperature in the grinding zone.

Since the grinding process was short-lived and the wear of the grinding wheel was insignificant, the cooling option was not included in the calculations.

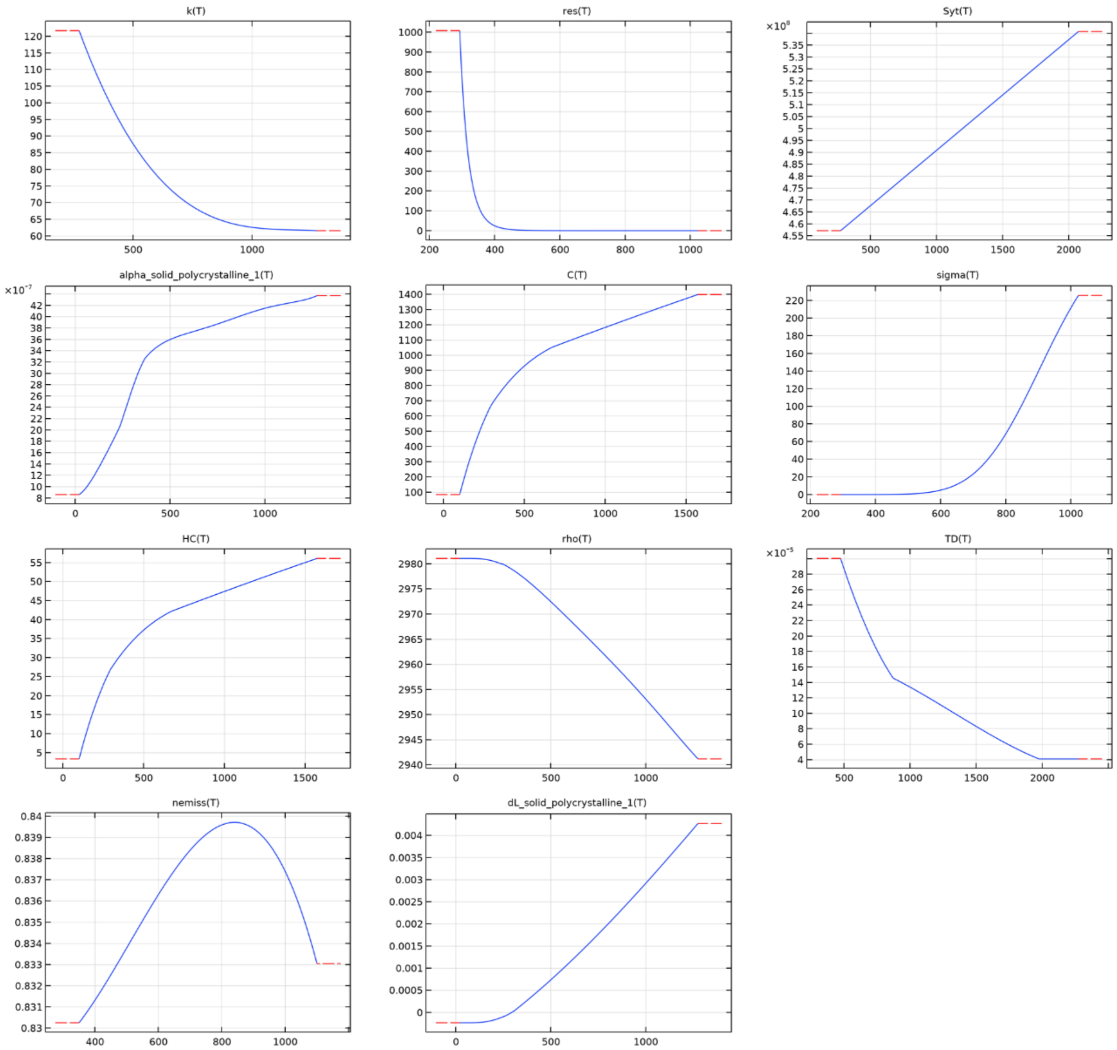

Figure 3. Properties of silicon carbide (grinding wheel) depending on temperature changes: *T* – temperature, *k* – thermal conductivity, *res* – resistivity, *Syt* – yield stress, *alpha_solid_polycrystalline_1* – coefficient of thermal expansion, *C* – heat capacity at constant pressure, *sigma* – electrical conductivity, *HC* – molar heat capacity, *rho* – density, *TD* – thermal diffusivity, *nemiss* – normal total emissivity, *dL_solid_polycrystalline_1* – thermal strain.

3. Results and discussion

The Figure 4 shows the distance that the rotating grinding wheel has moved relative to the workpiece being processed. The grinding wheel model moved 1.4 m relative to the workpiece model.

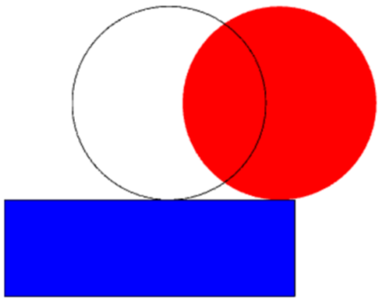

Figure 4. Displacement of the grinding wheel relative to the workpiece.

The results of the grinding process modeling, in the form of color contours that characterize the degree of stress-strain state of the workpiece model, are presented in the Figure 5. The stress-strain state was described by the calculated von Mises stress, pressure, and volumetric strain values. Below the model area, there is a scale that allows you to numerically determine the stress and strain parameters of the material being processed, with the lowest and highest values indicated. The calculated contours show that the entire volume of the steel workpiece is subjected to stress and strain. The minimum stress values are calculated away from the cutting zone, while the maximum values are calculated directly in the cutting zone. Significant stresses in the material are detected at a depth of up to ¼ of the accepted height of the workpiece.

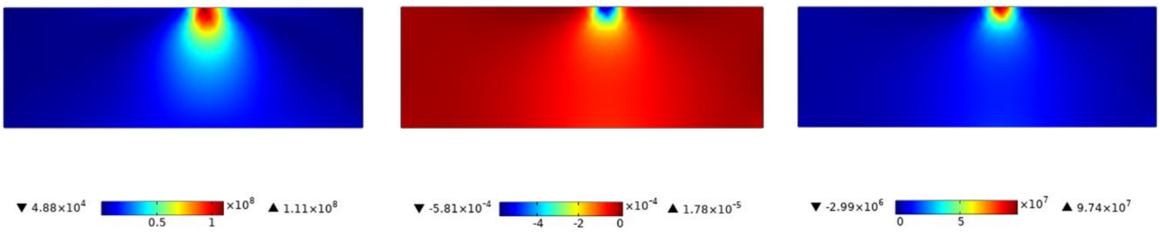

a ***b*** ***c***

Figure 5. Modeling results: *a* – von Mises stress (N/m^2); *b* – volumetric strain; *c* – pressure (N/m^2).

The nature of the workpiece material deformation can be judged by the numerical values of the volumetric strain coefficient. Material compression deformation (negative values of the volumetric strain coefficient) occurs directly in the contact zone between the grinding wheel and the workpiece. The workpiece material before and after the cutting zone undergoes tensile deformation. The tensile deformation of the material layers is twice as large as the compressive deformation of the layers.

The pressure contours determine the forces that occur during the flat grinding of the workpiece. The direction of the loads is determined by positive (compressive load) and negative (tensile load) pressure values. From this, we can conclude that the compressive force is an order of value greater than the tensile force.

The Figure 6 shows graphs of the calculated pressure measured in the longitudinal and transverse directions of the workpiece material.

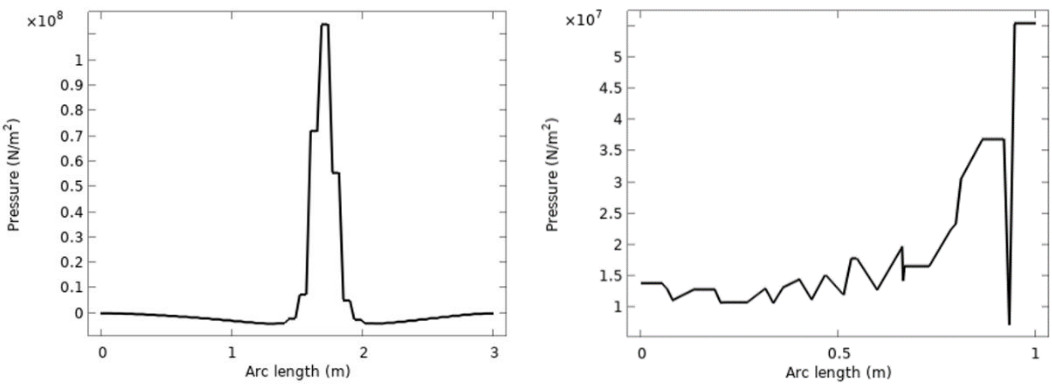

a ***b***

Figure 6. Dependence graphs: *a* – calculated pressure along the entire outer surface of the workpiece; *b* – calculated pressure measured in the cross-section of the workpiece relative to the grinding zone.

4. Conclusion

Based on the simulation results, the following conclusions can be drawn:

1. The effect of temperature in the grinding zone on the properties of 1010 low-carbon steel and silicon carbide has been determined. The differences in the change of physical, mechanical, and thermal properties of isotropic and anisotropic materials under temperature stress in the range of 500-800°C are noted. For example, the resistivity of steel increases, while it remains constant for silicon carbide.

2. Numerical values of stress intensity and strain during preliminary abrasive treatment of 1010 steel have been determined. Significant stresses in the material are detected at a depth of up to ¼ of the accepted height of the workpiece. In the cutting zone, compressive and tensile deformations are observed, caused by the corresponding forces. At the same time, a compressive force peak is determined in the cutting zone (the pressure is directed inward), and a certain area of the material before and after the cutting zone is subjected to tensile stress (negative pressure values that characterize the direction of pressure outward from the material).

References:

1. Marinescu, I. D., Hitchiner, M. P., Uhlmann, E., Rowe, W. B., & Inasaki, I. (2016). *Handbook of Machining with Grinding Wheels.* 2nd ed., CRC Press; Boca Raton, FL, USA.
2. Tyshkevich, V., Sukocheva, E., & Goncharova, E. (2017). Half-finished steel products flat grinding industrial efficiency increase. *Concept, No. 6*, 1-7.
3. Kruszyński, B. W., & Wójcik, R. (2001). Residual stress in grinding. *J. Mater. Process. Technol.*, *109*, 254-257.
4. Capello, E., & Semeraro, Q. (2002). Process parameters and residual stresses in cylindrical grinding. *J. Manuf. Sci. Eng.*, *124*, 615-623.
5. Ding, W., Zhang, L., Li, Z., Zhu, Y., Su, H., & Xu, J. (2017). Review on grinding-induced residual stresses in metallic materials. *Int. J. Adv. Manuf. Technol.*, *88*, 2939-2968.
6. Shen, S., Li, B., & Guo, W. (2020). Experimental study on grinding-induced residual stress in C-250 maraging steel. *Int. J. Adv. Manuf. Technol.*, *106*, 953-967.
7. Balart, M. J., Bouzina, A., Edwards, L., & Fitzpatrick, M. E. (2004). The onset of tensile residual stresses in grinding of hardened steels. *Mater. Sci. Eng. A.*, *367*, 132-142.
8. Nosov, N. V., et al. (2025). Mathematical Model of Residual Stress Formation during Flat Grinding with a Single Grain. *Russ. Engin. Res.*, *44*, 1804-1808.
9. Guo, G., Liu, Z., & An, Q. (2011). Experimental investigation on conventional grinding of Ti-6Al-4V using SiC abrasive. *Int. J. Adv. Manuf. Technol.*, *57(1-4)*, 135-142.
10. Barsukov, G. V., Vainer, L. G., Vasilenko, Yu. V., & Kozlov, A. M. (2011). *Modeling of technological processes of abrasive machining.* Moscow: Spectr.